DOI: 10.1002/cphc.201100133

IR Spectroscopy of Isolated Neutral and Protonated Adenine and 9-Methyladenine

Gydo C. P. van Zundert,[a] Sander Jaeqx,[a] Giel Berden,[a] Joost M. Bakker,[a] Karl Kleinermanns,[b] Jos Oomens,*[a, c] and Anouk M. Rijs*[a]

IR spectroscopy is employed to study isolated adenine and its derivative 9-methyladenine in both their neutral and protonated forms. The IR spectra of neutral adenine and 9-methyladenine are measured in a molecular beam expansion via IR–UV ion-dip spectroscopy in the 525 to 1750 cm^{-1} region. For adenine, UV excitation selects the 9H tautomer to give a conformer-selective IR spectrum. For 9-methyladenine, only one tautomer exists because of the methyl substitution at the N(9) position. The experimental spectra agree closely with spectra computed for these tautomers at the B3LYP/6-311++G(df,pd) level of theory. These spectra complement previous tautomer-specific IR spectra in the hydrogen stretching range. The 9H-adenine spectrum obtained is compared to a previously recorded FTIR spectrum of adenine at 280 °C, which shows close agreement, although the 7H tautomer cannot be excluded from contributing. Protonated adenine and 9-methyladenine are generated by electrospray ionization and studied via IR multiple-photon dissociation (IRMPD) spectroscopy. Comparison of the experimental spectra with computed spectra allows identification of the protonation site, which suggests that the 1-9 tautomer is the dominant contributor to the spectra.

1. Introduction

Owing to their biological importance, numerous experimental and theoretical studies have been devoted to the unraveling of the structural and photophysical properties of the individual nucleobases. In addition to its role as a nucleic acid building block, adenine and its derivatives are of interest in various other biochemical processes. For example, it is the main component of the energy-storing molecule adenosine triphosphate (ATP). In addition, its high photostability under UV irradiation is an intriguing property that has been suggested to be essential for the preservation of genetic information.[1] Furthermore, the various tautomeric forms of adenine have been under substantial scrutiny,[2–10] because of their proposed role in mutagenic and carcinogenic processes.[11–13]

To understand the fundamental principles behind its stability and the preference for certain tautomers, much effort has been devoted to the study of isolated adenine and its derivatives. Calculations at different levels of theory consistently showed 9H-adenine to be the most stable tautomer, followed by the 7H tautomer (see Figure 1), which is around 35 $kJ\,mol^{-1}$ higher in energy.[6,7,10,14–18] Some of the first IR spectra of adenine recorded in low-temperature inert gas matrices in the 400 to 4000 cm^{-1} range date back to 1985.[19] This study was extended by Nowak et al., who compared the experimental spectra with calculated IR frequencies at different levels of theory.[2,7,20–22] It was concluded that the absorption was due to the 9H tautomer.

Adenine in the gas phase has been studied by ultraviolet photoelectron spectroscopy,[23] microwave spectroscopy,[24] IR spectroscopy in a heated gas cell,[25] jet-cooled resonance-enhanced multiphoton ionization (REMPI) spectroscopy,[26–28] and IR–UV ion-dip spectroscopy.[5,8,29] In all of these studies, only the 9H tautomer was observed. However, based on comparison with jet-cooled IR–UV ion-dip spectroscopy in the NH stretching region and deuteration techniques, Plützer et al. suggested that the FTIR spectrum recorded in a gas cell at 280 °C contains a significant proportion of the 7H tautomer.[5,29]

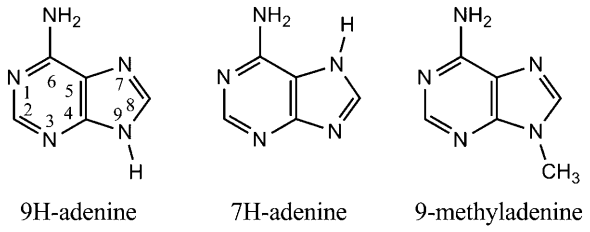

Figure 1. Chemical structures and atom numbering for the two tautomeric structures of adenine. For 9-methyladenine the N(9) position is blocked which inhibits tautomerization.

[a] G. C. P. van Zundert, S. Jaeqx, Dr. G. Berden, Dr. J. M. Bakker, Prof. Dr. J. Oomens, Dr. A. M. Rijs
FOM Institute for Plasma Physics Rijnhuizen
Edisonbaan 14, 3439 MN Nieuwegein (The Netherlands)
Fax: (+31) 30-6031204
E-mail: J.Oomens@Rijnhuizen.nl
A.M.Rijs@Rijnhuizen.nl

[b] Prof. Dr. K. Kleinermanns
Institut für Physikalische Chemie I
Heinrich-Heine-Universität
40225 Düsseldorf (Germany)

[c] Prof. Dr. J. Oomens
Van't Hoff Institute for Molecular Sciences
University of Amsterdam
Science Park 904, 1098 XH Amsterdam (The Netherlands)

Isolated 9-methyladenine, in which the N(9) position is substituted with a methyl group, has been experimentally investigated by numerous techniques, such as IR absorption spectroscopy in a low-temperature gas matrix,[19] REMPI spectroscopy,[27] and UV absorption in helium nanodroplets.[30] In addition, calculated vibrational spectra of the electronic ground state have been reported at several levels of theory.[15,31]

Since protonation can lead to structural changes and to proton-transfer-induced mutations, many experimental and theoretical studies have been carried out on protonated adenine in the gas phase to investigate changes in its photochemical and photophysical properties.[32–35] A combined experimental UV photofragmentation and theoretical study by Weinkauf et al. suggested protonation of 9H-adenine at the N(1) site (1-9-adenine).[33] Single and multiphoton UV-induced dissociation studies followed up on this.[34] The fragmentation patterns were similar to those obtained by collision-induced dissociation mass spectrometry, thus suggesting a statistical fragmentation process.[36] Very recently, UV-excitation-induced photofragmentation of protonated 1-9-adenine and 3-9-adenine was investigated.[32] Both tautomers exhibited rather similar fragmentation patterns and the fragmentation rate was similar for all fragments. IR multiple-photon dissociation (IRMPD) spectroscopy in the NH stretching region has been used to elucidate the structure of the protonated adenine dimer.[35] By comparing the experimental and calculated IR spectra, two dominant conformations were found.

Herein, we present the IR–UV ion-dip spectra (525–1750 cm^{-1}) of adenine and its 9-methyl derivative with the UV laser tuned to the π–π^* transition at 36106 and 36141 cm^{-1}, respectively.[26,27] To investigate the protonation site of adenine, the IRMPD spectra of protonated adenine (AH^+) and 9-methyladenine (9-MAH^+) are obtained in the 1000 to 1750 cm^{-1} range. To elucidate the tautomeric structure, the experimental IR spectra of both the neutral and protonated species are compared to computed harmonic vibrational frequencies at the B3LYP/6-311++G(df,pd) level of theory, which is known to give good results for adenine.[37] Furthermore, the measured spectrum of neutral adenine is compared to that observed in a heated gas cell by FTIR spectroscopy,[5] in order to discuss the possible presence of 7H-adenine.

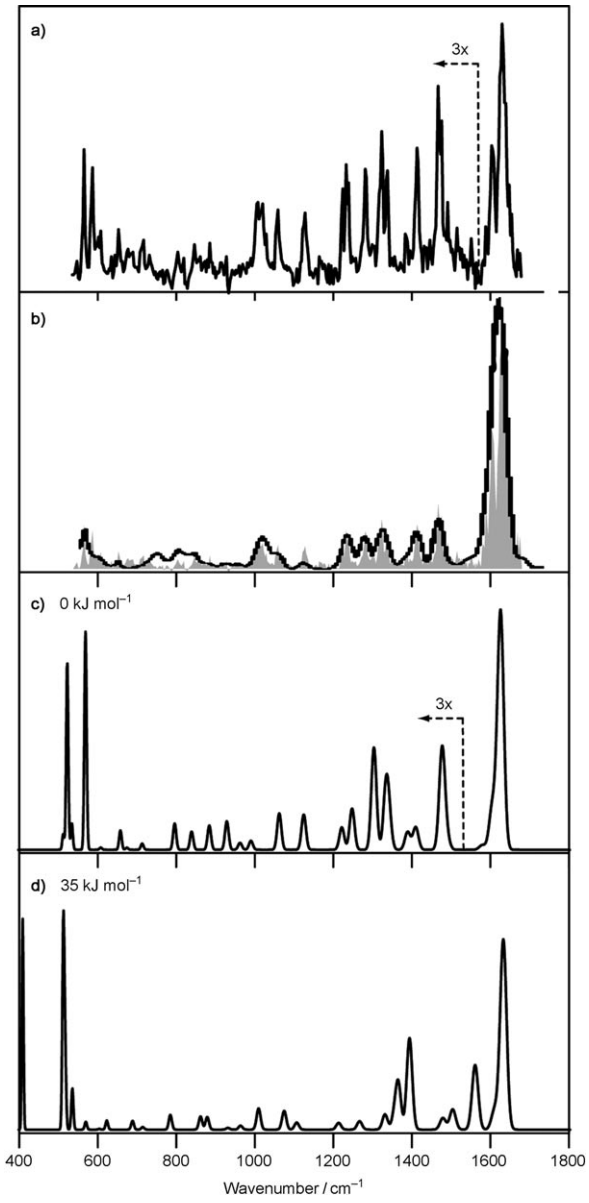

Figure 2. a) IR–UV ion-dip spectrum of adenine with the UV laser fixed on the 36106 cm^{-1} transition previously assigned to the 9H tautomer. b) FTIR spectrum of adenine at 280 °C taken from Plützer et al.; the IR–UV ion-dip spectrum of the 9H tautomer of (a) is shown as a gray silhouette. c, d) Calculated spectra of 9H-adenine (c) and 7H-adenine (d). The intensities in the spectral regions below about 1550 cm^{-1} are enlarged.

2. Results and Discussion

2.1. IR–UV Ion-Dip Spectroscopy

Figure 2a displays the IR absorption spectrum of adenine taken with the UV excitation laser fixed on the π–π^* transition at 36106 cm^{-1}. The IR spectrum obtained in the range from 500 to 1750 cm^{-1} shows a number of clear resonances, the line widths of which are mainly determined by the spectral resolution of FELIX (see Experimental Section). Fixing the UV excitation to other vibronic bands in the REMPI spectrum in the spectral range of 36050 to 36250 cm^{-1} reveals IR spectra with exactly the same frequencies and relative intensities.

Figure 2c and d show the theoretical spectra of 9H- and 7H-adenine, respectively. The calculated frequencies are scaled with a factor of 0.983 and convoluted with a Gaussian function mimicking the spectral profile of FELIX. General comparison of the experimental and theoretical spectra over the entire spectral range scanned shows that the theoretical spectrum of 9H-adenine resembles the measured spectrum more closely than that of 7H-adenine.

The strongest band in the IR spectrum found at 1630 cm^{-1} is associated with the NH_2 in-plane scissorlike bending vibration. The low-frequency shoulder of this resonance at 1603 cm^{-1} originates from the in-plane bending vibration of the N(9)-H group. The vibrational resonances at lower wavenumbers can be roughly divided into two classes: in the energy region between 1000 and 1500 cm^{-1}, vibrations can be

characterized as in-plane skeletal modes, whereas the region below 1000 cm^{-1} contains mainly vibrations of an out-of-plane nature, involving both hydrogen-bending and skeletal motions. A comparison of the experimental peak positions with the calculated frequencies is given in Table 1, and shows that the calculated spectrum of 9H-adenine is in very good agreement with the experimental spectrum.

Table 1. Measured IR–UV ion-dip frequencies and assigned computed modes of 9H-adenine and 9-methyladenine. For completeness, the 7H-adenine frequencies are presented as well. The peak positions are given in cm^{-1}.

9H-adenine			7H-adenine		9-methyladenine		
IR–UV	Calc.[a]	Mode description[b]	Calc.[a]	Mode description[b]	IR–UV	Calc.[a]	Mode description[b]
1630	1625	$\delta_{sciss}NH_2$, $\nu(C_5–C_6)$, $\nu(C_6–N_6)$	1631	$\delta_{sciss}NH_2$, $\nu(C_5–C_6)$, δN_7H	1632	1627	$\delta_{sciss}NH_2$, $\nu(N_1–C_2)$, $\nu(C_5–C_6)$, $\nu(C_6–N_6)$
1603	1604	$\nu(N_3–C_4)$, $\nu(C_5–C_6)$, $\nu(N_7–C_8)$, δN_9H, δC_8H	1609	$\delta_{sciss}NH_2$	1599	1593	$\delta_{sciss}NH_2$, $\nu(N_1–C_6)$, $\nu(N_3–C_4)$, $\nu(C_5–C_6)$, δC_8H, $defCH_3$
1588	1578	$\delta_{sciss}NH_2$, δC_2H	1559	$\delta_{sciss}NH_2$, $\nu(N_1–C_6)$, $\nu(N_3,C_4)$, δC_2H		1579	$\delta_{sciss}NH_2$, $\nu(N_1–C_2)$, $\nu(C_4–C_5)$
1515					1515	1507	$\delta_{sciss}NH_2$, δC_8H, $\nu(C_5–C_6)$, $\nu(N_7–C_8)$, $\nu(N_9–C_9)$, $defCH_3$
1491	1498	$\delta_{sciss}NH_2$, $\nu(N_7–C_8)$, δC_8H	1502	δN_6H, $\nu(C_5–C_6)$, δN_7H, δC_8H, $\nu(C_8–N_9)$		1490	$defCH_3$
1476	1476	δC_2H, $\delta_{sciss}NH_2$, δC_8H, δN_9H, $\nu(N_1–C_6)$, $\nu(C_2–N_3)$, $\nu(C_6–N_6)$	1477	δC_2H, $\nu(N_1–C_6)$, δN_6H, δN_7H	1470	1473	$\delta_{sciss}NH_2$, δC_2H, $\nu(C_6–N_6)$, $defCH_3$
1467					1450	1456	$defCH_3$
1413	1408	δC_2H, $\nu(C_4–C_5)$, $\nu(C_6–N_6)$, $\nu(C_4–N_9)$, δN_6H, δC_8H, δN_9H	1392	δN_7H, $\nu(N_7–C_8)$, δC_8H	1429	1439	$defCH_3$, $\nu(N_7–C_8)$, δC_8H, $\nu(C_5–N_9)$
1383	1388	δN_9H, δC_2H, $\nu(C_4–N_9)$	1364	δC_2H, $\nu(C_4–C_5)$, δC_8H	1414	1415	$defCH_3$, δN_6H, $\nu(C_6–N_6)$, δC_2H, $\nu(C_5–N_9)$, $\nu(N_7–C_8)$
1338	1340	δC_2H, δN_9H, δC_8H, δN_6H, $\nu(C_8–C_9)$, $\nu(C_6–N_6)$	1354	δC_8H, $\delta_{sciss}NH_2$, $\nu(C_4–N_9)$	1369	1369	δC_2H, $\nu(C_6–N_6)$, $\nu(C_4–C_5)$
1323	1333	$\nu(N_1–C_2)$, $\nu(C_5–N_7)$, $\nu(C_4–C_5)$, δC_2H, δC_8H, δN_6H	1330	δC_2H, δN_6H	1345	1341	$\delta_{sciss}NH_2$, δ_{def}6-ring, δ_{def}5-ring, $defCH_3$
1281	1302	$\nu(N_1–C_2)$, $\nu(C_2–N_3)$, $\nu(C_5–C_6)$, $\nu(C_5–N_7)$, δC_2H, δN_9H	1284	$\delta_{rock}NH_2$, δ_{def}6-ring	1327	1336	δC_2H, $\nu(C_5–N_7)$ $\nu(N_1–C_2)$, $\nu(C_8–N_9)$, δC_8H, $defCH_3$
1239	1247	δC_8H, δN_9H, δC_2H	1265	δC_8H, δC_2H, δN_6H, δN_7H	1292	1307	$\delta_{rock}NH_2$, δ_{def}6-ring, δC_8H
1233					1268		
1224	1221	$\delta_{rock}NH_2$, δC_2H, δC_8H, $\nu(N_1–C_2)$, $\nu(C_2–N_3)$, $\nu(C_5–N_7)$	1212	$\delta_{rock}NH_2$, δN_7H, δC_8H	1256	1254	$\delta_{rock}NH_2$, $\nu(N_1–C_2)$, δC_2H, $\nu(C_5–N_7)$, δC_8H
1128	1124	δN_6H, δC_2H, δC_8H, δN_9H, $\nu(N_3–C_4)$, $\nu(C_4–N_9)$, $\nu(C_5–N_7)$	1105	$\delta_{rock}NH_2$, δN_7H, δC_2H, δC_8H	1232	1241	δC_8H, δN_6H, δC_2H, $defCH_3$
1059	1062	δC_8H, δN_9H, $\nu(C_8–N_9)$	1073	δN_7H, δC_8H, δN_6H	1199	1199	$\delta_{rock}NH_2$, δ_{str}6-ring, $\nu(C_5–N_7)$, $\nu(N_9–C_9)$, δC_8H
1020	990[c]	$\delta_{rock}NH_2$, $\nu(N_1–C_6)$, δC_2H	1008	$\delta_{rock}NH_2$, δC_2H	1136	1131	$defCH_3$
1008					1067	1055	$\delta_{rock}NH_2$, $\nu(C_4–N_9)$, $defCH_3$
	962	γC_2H	962	γC_2H	1036	1041	$\delta_{rock}NH_2$, δC_8H, $\nu(C_8–N_9)$, $defCH_3$
928	928	δ_{def}5-ring, $\nu(C_4–C_5)$, δN_6H, $\nu(N_1–C_6)$, δC_2H	930	δ_{def}5-ring, $\nu(C_4–C_5)$	1000	984	$\delta_{rock}NH_2$, $\nu(N_1–C_6)$, δC_2H
885	884	δ_{def}6-ring, $\nu(C_4–N_9)$, $\nu(C_5–N_7)$, δC_8H, δN_9H, δN_6H	877	δ_{def}6-ring, $\nu(C_4–N_9)$, $\nu(C_5–N_7)$, δC_8H	976		
846	839	γC_8H	860	γC_8H	958	961	γC_2H
819					895	892	δ_{def}6-ring, δ_{def}5-ring, δN_6H, δC_8H, $rockCH_3$
804	795	τ_{def}6-ring, τ_{def}5-ring, $\gamma(C_6–N_6)$	784	τ_{def}6-ring, τ_{def}5-ring,	841	838	γC_8H
777					800	796	τ_{def}6-ring, τ_{def}5-ring
732					730	734	δ_{def}6-ring, δ_{def}5-ring, $\nu(N_9–C_9)$
717	712	δ_{str}6-ring, δ_{str}5-ring, $\nu(C_6–N_6)$, δN_6H	713	δ_{str}6-ring, δ_{str}5-ring, $\nu(C_6–N_6)$, δN_6H	715	718	δ_{str}6-ring, δ_{str}5-ring, $rockCH_3$
689					694		
677	674	$\gamma(C_6–N_6)$, τ_{def}6-ring, τ_{def}5-ring	687	τ_{def}6-ring, τ_{def}5-ring, $\gamma(C_6–N_6)$	673	679	τ_{def}6-ring, τ_{def}5-ring, $\gamma(C_6–N_6)$, $defCH_3$
653	657	τ_{def}5-ring, τ_{def}6-ring	622	τ_{def}5-ring, τ_{def}6-ring	667		
635					640	650	τ_{def}6-ring, τ_{def}5-ring, γN_6H
608	607	δ_{def}6-ring, δ_{def}5-ring, δN_6H	603	δ_{def}6-ring, δ_{def}5-ring, δN_6H	592		
587					577	578	δNH_2, $\nu(C_5–C_6)$, δC_8H
565	569	τ_{def}6-ring, τ_{def}5-ring, γN_6H	568	γC_2H, τ_{def}6-ring, τ_{def}5-ring	571		
547					553	558	τ_{def}6-ring, τ_{def}5-ring

[a] Calculations performed at the B3LYP/6-311++G(df,pd) level of theory. Scaling factor used was 0.982 for adenine and 0.983 for 9-methyladenine. [b] Abbreviations: ν = stretch; δ = in-plane bend; γ = out-of-plane bend; τ = torsional; sciss = scissoring; rock = rocking; str = stretch; def = deformation. [c] Assignment based on the calculated anharmonic frequency by Zierkiewicz et al.[37]

The relatively intense band at 587 cm^{-1} is not predicted by our calculations. The same mismatch with theory is observed in the low-temperature argon matrix spectrum where a doublet appears at 591 and 583 cm^{-1}.[2] Xue et al. assigned these bands to the NH_2 torsion twisting vibration,[31] while Santamaria et al. attributed them to the NH_2 rocking vibration.[38] Zierkiewicz et al. showed that the previous assignments were erroneous and agreed with the suggestion made by Nowak et al. that the doublet does not correspond to a fundamental transition but probably corresponds to the overtone of the NH_2-inversion mode.[2,37] The intensity enhancement of the overtone is due to the anharmonic nature of the vibrational potential, as was for instance also found, and discussed in much detail, for the molecular beam IR spectrum of aniline.[39] In line with these observations we assign the 587 cm^{-1} band to the overtone of the NH_2-inversion mode.

Computations indicate that 9H-adenine is energetically favored over the 7H-adenine tautomer by 35 $kJ\,mol^{-1}$. This further confirms that it is the 9H-adenine tautomer that is observed in the experiment, which is also consistent with previous assignment of the REMPI spectrum and measurements in the 3 μm IR range.[8]

Figure 2b shows the FTIR spectrum of adenine recorded in a heated gas cell at 280 °C taken from Plützer et al.[5] with our experimental IR–UV ion-dip spectrum of 9H-adenine overlaid as a gray silhouette. It is clear that the FTIR spectrum in the mid-IR region closely resembles the IR–UV ion-dip spectrum of 9H-adenine. No additional bands are observed and the relative intensities are very similar, which suggests that the 9H tautomer dominates the population in the heated gas cell. However, a substantial contribution of the 7H tautomer, as suggested previously based on ion-dip spectra in the NH stretching range, cannot be excluded here, mainly because a 7H-adenine tautomer-specific IR spectrum is not available in the 500–1750 cm^{-1} region. The low ion signal at the strongest transition in the UV spectrum of the 7H tautomer at 35824 cm^{-1}[5] under our experimental conditions prevented us from recording such a spectrum. The near-IR FTIR spectrum of adenine resembles more closely the IR–UV spectrum taken at 35824 cm^{-1}.[5,25] Based on the calculated spectrum for the 7H-adenine tautomer in the mid-IR region (Figure 2d), a substantial contribution of this tautomer appears unlikely, judging for instance by the absence of an absorption around 1555 cm^{-1} in the FTIR spectrum. However, the calculated spectrum may not accurately predict the relative intensities, as is for instance seen by comparison of the experimental and theoretical spectra for the 9H tautomer (Figure 2a and c). The apparently distinct conclusions based on the IR–UV ion-dip spectra recorded in both the near-IR[5] as well as the mid-IR region (presented here) remain somewhat puzzling, though variations in experimental conditions in the various studies, the possible dissimilar absorption cross section for the 7H- and 9H-adenine, as well as inaccuracies in the calculated spectra used to assign the experimental spectra cannot be excluded.

The IR–UV ion-dip spectrum of 9-methyladenine recorded in the spectral range from 500 to 1750 cm^{-1} at the 36141 cm^{-1} transition is depicted in Figure 3 together with its calculated

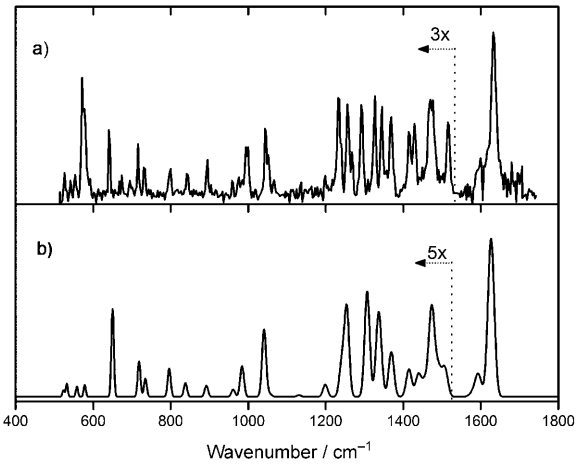

Figure 3. a) IR–UV ion-dip spectrum of 9-methyladenine at the π–π* transition at 36141 cm^{-1} and b) its calculated spectrum. The bands below 1550 cm^{-1} are enlarged.

spectrum. The experimental spectrum shows many resolved bands and is roughly analogous to the spectrum of 9H-adenine, with one dominant band at 1632 cm^{-1} and a shoulder at 1599 cm^{-1}. As in the spectrum of 9H-adenine, roughly two regions can be distinguished in the spectrum, that is, a region with in-plane modes above 1000 cm^{-1} and one with predominantly out-of-plane skeletal modes at lower frequencies. Moreover, some additional bands are present, mainly in the 1000 to 1500 cm^{-1} range, which correspond to deformations of the methyl group.

A relatively intense band is observed at 571 cm^{-1}, similar to the 587 cm^{-1} band in adenine. Even though for 9-methyladenine there is a fundamental vibration calculated at 578 cm^{-1}, the intensity mismatch is so pronounced that we assign the 571 cm^{-1} band to the overtone of the NH_2-inversion mode. Further assignments of the calculated with the measured frequencies are given in Table 1.

2.2. Protonated Adenine and 9-Methyladenine

The IRMPD spectra of protonated adenine (AH^+) and 9-methyladenine (9-MAH^+) obtained in the spectral range from 1000 to 1750 cm^{-1} are presented in Figure 4 and Figure 5, respectively. Upon IR activation, protonated adenine (*m/z* 136) was found to fragment into *m/z* 119 (loss of NH_3), *m/z* 109 (loss of HCN), and *m/z* 94 (loss of NH_2CN) in accordance with previous UV photofragmentation studies.[32–34] The IRMPD yield in the 119, 109, and 94 mass channels is summed and divided by the laser fluence, and plotted against photon energy giving the IRMPD spectrum shown in Figure 4. The IRMPD spectrum of adenine shows one dominant feature consisting of a peak at 1653 cm^{-1} with a shoulder on the low-frequency side at 1605 cm^{-1}. These bands originate from scissor modes of the NH_2 group. Below 1500 cm^{-1} a few small features appear in the spectrum resulting from various in-plane bending modes.

The assignment of the IRMPD spectra of protonated adenine is based on the comparison with the calculated spectra of dif-

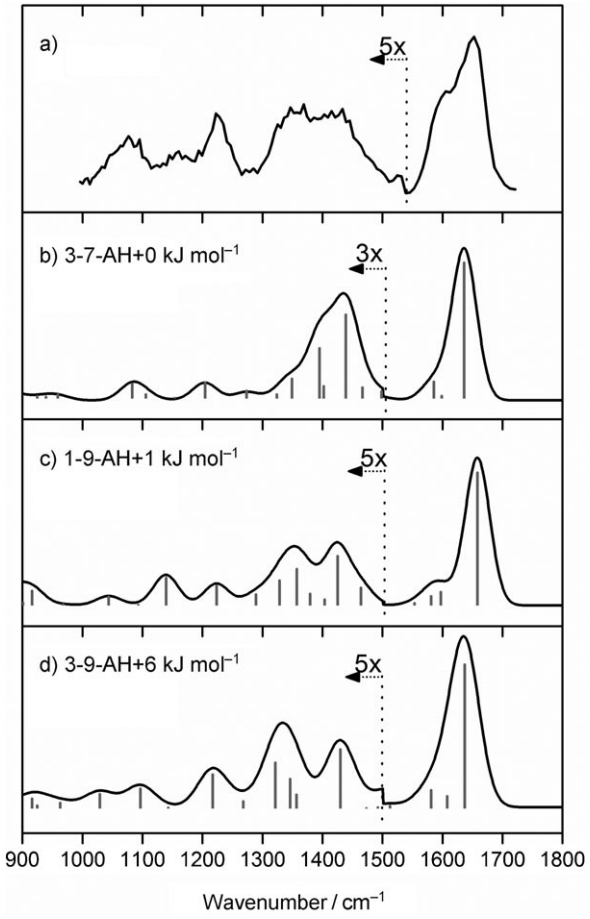

Figure 4. a) IRMPD spectrum of protonated adenine compared with b–d) the calculated spectra of the three lowest-energy tautomers. The bars under the graphs are the calculated modes. Below 1500 cm^{-1} the graphs are enlarged for better comparison.

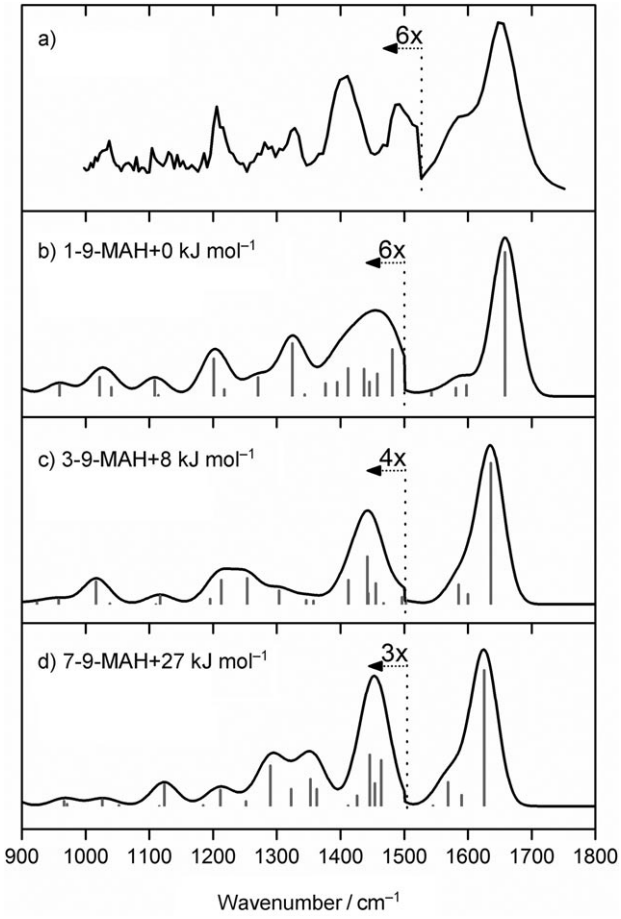

Figure 5. a) IRMPD spectrum of protonated 9-methyladenine together with b–d) calculated spectra of the three possible tautomers. Bars under the calculated graphs represent the modes. Graphs are enlarged below 1500 cm^{-1} for better comparison.

ferent low-energy tautomeric structures. The calculated spectra are convoluted with a 50 cm^{-1} full width at half maximum (FWHM) Gaussian function and the calculated frequencies are scaled with a factor of 0.968. The three tautomers are found to lie very close in energy. The 3-9-AH^+ is only 6 kJ mol^{-1} higher in energy than 3-7-AH^+, which is practically isoenergetic with the 1-9-AH^+ tautomer. Other tautomers are calculated to be more than 34 kJ mol^{-1} higher in energy and are not considered here. Due to the presence of three conformations within 6 kJ mol^{-1}, superposition of the IR spectra of 1-9-AH^+ and 3-7-AH^+ and possibly 3-9-AH^+ may be expected at the temperature of the Fourier transform ion cyclotron resonance (FTICR) trap (293 K). However, specific spectral features, such as the shoulder at 1600 cm^{-1} and the weak broad absorption between 1300 and 1500 cm^{-1}, are both best reproduced by the theoretical 1-9-AH^+ spectrum. The 1600 cm^{-1} shoulder is not nearly as pronounced in the spectra calculated for the 3-9-AH^+ and 3-7-AH^+ tautomers. Moreover, the 3-7-AH^+ calculation does not reproduce the 1300 to 1500 cm^{-1} range as well as the calculation for the 1-9-AH^+ tautomer. Although the presence of 3-9-AH^+ and 3-7-AH^+ cannot be excluded based on the experimental spectrum, the dominant species appears to be the 1-9-AH^+.

The presence of only 1-9-AH^+ in the gas phase, even though 3-7-AH^+ is nearly isoenergetic, has been attributed by Marian et al. to artifacts inherent to electrospray ionization (ESI).[33] In the water/methanol solution used for ESI, certain tautomers are stabilized more than others. Upon transfer to the gas phase the tautomeric distribution does not change significantly since the exchange of two hydrogen atoms is relatively slow. Consequently, the energy calculations on isolated molecules can predict different tautomers to be the most stable structure. Indeed, calculations with one added water molecule show that the 1-9 tautomer is significantly lower in energy than the other structures.[33]

The fragments of 9-MAH^+ (*m/z* 150) after IR irradiation were found at *m/z* 133 (loss of NH_3), *m/z* 123 (loss of HCN), and *m/z* 108 (loss of NH_2CN). The IRMPD spectrum of 9-MAH^+, obtained by summing the fragmentation yield in these mass channels, shows the same features as AH^+. The dominant spectral feature is found at 1650 cm^{-1} with a shoulder at 1585 cm^{-1}, which corresponds to NH_2 scissor vibrations. Bands of lower intensity are seen below 1530 cm^{-1} and are attributed to in-plane vibrations of the purine moiety and deformations of the methyl group.

Assigning the dominant tautomeric structure of 9-MAH$^+$ is more straightforward than for AH$^+$, since fewer tautomers are possible. Moreover, the energy differences are larger for 9-MAH$^+$ tautomers. The most stable structure is the 1-9 tautomer followed by 3-9-MAH$^+$ at 8 kJ mol^{-1} and 7-9-MAH$^+$ at 27 kJ mol^{-1}. Comparison of the calculated spectra with the IRMPD spectrum shows that the calculated spectrum of 1-9-MAH$^+$ provides the closest match to the experimental spectrum. The shoulder around 1585 cm^{-1} is prominently present and there is excellent agreement below 1350 cm^{-1}. Thus, we conclude that the dominant tautomer present is the 1-9-MAH$^+$ structure, although minor contributions of other tautomers cannot be excluded.

3. Conclusions

The IR absorption spectra of the nucleobase adenine and its derivative 9-methyladenine were measured under isolated conditions in the gas phase. IR–UV ion-dip spectroscopy was applied to study the neutral species, while IRMPD was employed to examine their protonated forms. The IR spectra of neutral adenine and 9-methyladenine contain a large number of well-resolved resonances. For adenine, comparison of the experimental and calculated spectra confirms the presence of 9H-adenine. In addition, the FTIR spectrum of adenine recorded previously closely resembles the experimental IR–UV ion-dip spectrum in this frequency range, although the presence of the 7H tautomer in the gas-phase sample cannot be excluded.

The IRMPD spectrum of protonated adenine in the 1000 to 1750 cm^{-1} region shows features that match particularly well with the calculated spectrum of 1-9-AH$^+$. Although other tautomers cannot be excluded, gas-phase protonated adenine produced via ESI is suggested to exist mainly in the 1-9 tautomer form, which is consistent with earlier observations.[33] The IRMPD spectrum of protonated 9-methyladenine also indicates the presence of mainly the 1-protonated tautomer.

Experimental Section

Neutral Adenine and 9-Methyladenine: The IR–UV ion-dip spectra of neutral adenine and 9-methyladenine were obtained using a pulsed molecular beam setup equipped with a laser-desorption source and a reflectron time-of flight (TOF) mass spectrometer.[40,41] Samples of adenine (99%) and 9-methyladenine (97%) (Sigma–Aldrich) were used without further purification. A mixture of the sample and graphite powder was applied onto the surface of a bar of solid graphite ($50\times15\times1$ mm^3). The sample bar was placed on a translatable stage to provide fresh sample every laser shot, directly under the orifice of a pulsed valve. The 10 Hz pulsed valve released gas pulses of argon (typically 60 μs long) through a 0.5-mm-diameter nozzle into a vacuum at a backing pressure of 3.5 bar. Directly after opening the nozzle a pulsed Nd:YAG laser (Polaris II, New Wave Research) operating at 10 Hz, 1064 nm, and 1 mJ per pulse desorbed sample molecules from the graphite matrix. The neutral, gas-phase molecules were entrained and vibrationally cooled in the supersonic expansion of argon. About 10 cm downstream from the source the molecular beam was skimmed and entered the differentially pumped chamber housing the TOF mass spectrometer (Jordan Co.). In the extraction zone, the molecules in the beam were electronically excited and ionized by UV radiation from a 10 Hz Nd:YAG (Innolas GmbH, Spitlight 1200) pumped frequency-doubled dye laser (Radiant Dyes, NarrowScan). The dye laser operating on Coumarin 153 generated tunable UV radiation in the 36000–36300 cm^{-1} region with a typical pulse energy of 2.5 mJ. The resulting ions were accelerated towards a microchannel-plate (MCP) detector, thereby yielding mass spectra with a resolution of $M/\Delta M = 2000$.

IR–UV ion-dip spectroscopy was employed to obtain the IR absorption spectra of jet-cooled adenine and 9-methyladenine. The ions were constantly produced from ground-state molecules by using a $(1+1)$ two-photon ionization scheme. About 500 ns prior to the excitation and the ionization beam, the IR laser interacted with the molecular beam. If the IR laser was resonant with a vibrational transition, population was transferred from the ground state into the vibrationally excited state, which led to a depletion of the ground-state population. This resulted in a decrease in the number of produced adenine/9-methyladenine ions. By measuring the ion yield of the mass of interest while varying the wavelength of the IR laser, the IR ion-dip spectrum was obtained. The spectrum was recorded in the frequency range between 500 and 1750 cm^{-1}, using the radiation produced by the Free Electron Laser for Infrared eXperiments (FELIX) located at our institute.[42] FELIX produces an approximately 5-μs-long burst (macropulse) of micropulses. The micropulse spacing within the burst is 1 ns. The micropulse duration is set to about 100 optical cycles, which results in a spectral bandwidth of approximately 0.5% (FWHM) of the central frequency. Typically, energies of up to 60 mJ are reached in the macropulse. The frequency range that can be covered extends from 40 to 2000 cm^{-1} although only the range from 500 to 1750 cm^{-1} is used in the present study. In the experiment, the UV excitation/ionization laser and the molecular beam ran at a 10 Hz repetition rate, while FELIX operated at 5 Hz. By independently recording the alternating IR-on and IR-off signals, a normalized ion-dip spectrum could be obtained, which was insensitive to long-term drifts in UV laser power or source conditions. Additionally, the IR spectra were corrected for the intensity variations of the IR energy over the complete wavelength range.

Protonated Adenine and 9-Methyladenine: Protonated adenine and 9-methyladenine were generated by ESI (Micromass/Waters Z-spray source) using a 1 mM solution of the sample in an 80:20 methanol/water mixture, with a few drops of acetic acid (>99%, Fluka) added to aid the protonation of the nucleobase. The produced ions were accumulated in a linear hexapole trap before they were pulse-injected into the FTICR ion trap equipped with a 4.7 T actively shielded superconducting magnet (Cryomagnetics Inc.).[43–45] In the ICR cell, the ion of interest was mass-isolated using a stored waveform inverse Fourier transform (SWIFT) excitation pulse.[46] The mass-selected ions were then irradiated with the focused output of the free-electron laser FELIX.[42] To produce the IR spectra, the wavelength of FELIX was scanned between 1000 and 1750 cm^{-1}, and the fragment and parent ion intensities were measured at each step using the excite/detect sequence. At each wavelength, three mass spectra were averaged, and the IRMPD yield was linearly corrected for the variations in the FELIX power over the complete spectral range.

Calculations: All quantum-chemical calculations were performed using the Gaussian 03 program package.[47] Calculation of the harmonic vibrational frequencies of the ground states was done by using the analytical second derivatives at the B3LYP/6–311++G(df,pd) level of theory.[48–50] Scaling factors for the neutral species were calculated by assigning a structure to the experimental spec-

trum, after which a linear regression was performed between the assigned calculated and experimental frequencies. For adenine the resulting scaling factor was 0.982 and for 9-methyladenine 0.983. The scaling factor used for the protonated species was 0.968 based on the recommendations by Andersson and Uvdal.[51] Energies given are zero-point-energy corrected. Furthermore, the calculated spectra were convoluted with a Gaussian profile representing the bandwidth of FELIX for IR–UV ion-dip spectroscopy. For the protonated species, spectra were convoluted with a 50 cm^{-1} FWHM profile for comparison with the experimental IRMPD spectra.

Acknowledgements

The skillful assistance of the FELIX staff is gratefully acknowledged. This work is part of the research program of FOM, which is financially supported by the Nederlandse Organisatie voor Wetenschappelijk Onderzoek (NOW).

Keywords: conformational analysis · density functional calculations · IR spectroscopy · nucleobases · tautomerism

[1] C. E. Crespo-Hernández, B. Cohen, P. M. Hare, B. Kohler, *Chem. Rev.* **2004**, *104*, 1977.
[2] M. J. Nowak, L. Lapinski, J. S. Kwiatkowski, J. Leszczynski, *J. Phys. Chem.* **1996**, *100*, 3527.
[3] S. K. Mishra, M. K. Shukla, P. C. Mishra, *Spectrochim. Acta A* **2000**, *56*, 1355.
[4] A. Laxer, D. T. Major, H. E. Gottlieb, B. Fischer, *J. Org. Chem.* **2001**, *66*, 5463.
[5] C. Plützer, K. Kleinermanns, *Phys. Chem. Chem. Phys.* **2002**, *4*, 4877.
[6] J. S. Kwiatkowski, J. Leszczynski, *THEOCHEM* **1990**, *67*, 35.
[7] M. J. Nowak, H. Rostkowska, L. Lapinski, J. S. Kwiatkowski, J. Leszczynski, *J. Phys. Chem.* **1994**, *98*, 2813.
[8] C. Plützer, E. Nir, M. S. de Vries, K. Kleinermanns, *Phys. Chem. Chem. Phys.* **2001**, *3*, 5466.
[9] L. M. Salter, G. M. Chaban, *J. Phys. Chem. A* **2002**, *106*, 4251.
[10] M. Hanus, M. Kabelac, J. Rejnek, F. Ryjacek, P. Hobza, *J. Phys. Chem. B* **2004**, *108*, 2087.
[11] M. D. Topal, J. R. Fresco, *Nature* **1976**, *263*, 285.
[12] V. H. Harris, C. L. Smith, W. J. Cummins, A. L. Hamilton, H. Adams, M. Dickman, D. P. Hornby, D. M. Williams, *J. Mol. Biol.* **2003**, *326*, 1389.
[13] V. I. Danilov, V. M. Anisimov, C. Kurita, D. Hovorun, *Chem. Phys. Lett.* **2005**, *412*, 285.
[14] U. Norinder, *THEOCHEM* **1987**, *151*, 259.
[15] J. Wiorkiewicz-Kuczera, M. Karplus, *J. Am. Chem. Soc.* **1990**, *112*, 5324.
[16] M. Sabio, S. Topiol, W. C. Lumma, *J. Phys. Chem.* **1990**, *94*, 1366.
[17] C. Fonseca Guerra, F. M. Bickelhaupt, S. Saha, F. Wang, *J. Phys. Chem. A* **2006**, *110*, 4012.
[18] A. Sygula, A. Buda, *THEOCHEM* **1983**, *92*, 267.
[19] S. G. Stepanian, G. G. Sheina, E. D. Radchenko, Y. P. Blagoi, *J. Mol. Struct.* **1985**, *131*, 333.
[20] M. J. Nowak, L. Lapinski, J. S. Kwiatkowski, *Chem. Phys. Lett.* **1989**, *157*, 14.
[21] M. J. Nowak, L. Lapinski, J. S. Kwiatkowski, J. Leszczynski, *Spectrochim. Acta Part A* **1991**, *47*, 87.
[22] M. J. Nowak, H. Rostkowska, L. Lapinski, J. S. Kwiatkowski, J. Leszczynski, *Spectrochim. Acta Part A* **1994**, *50*, 1081.
[23] J. Lin, C. Yu, S. Peng, I. Akiyama, K. Li, L. K. Lee, P. R. LeBreton, *J. Am. Chem. Soc.* **1980**, *102*, 4627.
[24] R. D. Brown, P. D. Godfrey, D. McNaughton, A. P. Pierlot, *Chem. Phys. Lett.* **1989**, *156*, 61.
[25] P. Colarusso, K. Zhang, B. Guo, P. F. Bernath, *Chem. Phys. Lett.* **1997**, *269*, 39.
[26] N. J. Kim, G. Jeong, Y. S. Kim, J. Sung, S. K. Kim, Y. D. Park, *J. Chem. Phys.* **2000**, *113*, 10051.
[27] D. C. Lührs, J. Viallon, I. Fischer, *Phys. Chem. Chem. Phys.* **2001**, *3*, 1827.
[28] E. Nir, K. Kleinermanns, L. Grace, M. S. de Vries, *J. Phys. Chem. A* **2001**, *105*, 5106.
[29] E. Nir, C. Plützer, K. Kleinermanns, M. S. de Vries, *Eur. Phys. J. D* **2002**, *20*, 317.
[30] S. Smolarek, A. M. Rijs, W. J. Buma, M. Drabbels, *Phys. Chem. Chem. Phys.* **2010**, *12*, 15600.
[31] Y. Xue, D. Xie, G. Yan, *Int. J. Quantum Chem.* **2000**, *76*, 686.
[32] N. R. Cheong, S. H. Nam, H. S. Park, S. Ryu, J. K. Song, S. M. Park, M. Perot, B. Lucas, M. Barat, J. A. Fayeton, C. Jouvet, *Phys. Chem. Chem. Phys.* **2011**, *13*, 291.
[33] C. Marian, D. Nolting, R. Weinkauf, *Phys. Chem. Chem. Phys.* **2005**, *7*, 3306.
[34] D. Nolting, R. Weinkauf, I. V. Hertel, T. Schultz, *ChemPhysChem* **2007**, *8*, 751.
[35] K. Rajabi, K. Theel, E. A. L. Gillis, G. Beran, T. D. Fridgen, *J. Phys. Chem. A* **2009**, *113*, 8099.
[36] C. C. Nelson, J. A. McCloskey, *J. Am. Chem. Soc.* **1992**, *114*, 3661.
[37] W. Zierkiewicz, L. Komorowski, D. Michalska, J. Cerny, P. Hobza, *J. Phys. Chem. B* **2008**, *112*, 16734.
[38] R. Santamaria, E. Charro, A. Zacarias, M. Castro, *J. Comput. Chem.* **1999**, *20*, 511.
[39] H. Piest, G. von Helden, G. Meijer, *J. Chem. Phys.* **1999**, *110*, 2010.
[40] A. M. Rijs, N. Sandig, M. N. Blom, J. Oomens, J. S. Hannam, D. A. Leigh, F. Zerbetto, W. J. Buma, *Angew. Chem.* **2010**, *121*, 3988; *Angew. Chem. Int. Ed.* **2010**, *49*, 3896.
[41] H. Zhu, M. Blom, I. Compagnon, A. M. Rijs, S. Roy, G. von Helden, B. Schmidt, *Phys. Chem. Chem. Phys.* **2010**, *12*, 3415.
[42] D. Oepts, A. F. G. Van der Meer, P. W. Van Amersfoort, *Infrared Phys. Technol.* **1995**, *36*, 297.
[43] T. H. Mize, I. Taban, M. Duursma, M. Seynen, M. Konijnenburg, A. Vijftigschild, C. V. Doornik, G. V. Rooij, R. M. A. Heeren, *Int. J. Mass Spectrom.* **2004**, *235*, 243.
[44] N. C. Polfer, J. Oomens, *Phys. Chem. Chem. Phys.* **2007**, *9*, 3804.
[45] J. J. Valle, J. R. Eyler, J. Oomens, D. T. Moore, A. F. G. van der Meer, G. von Helden, G. Meijer, C. L. Hendrickson, A. G. Marshall, G. T. Blakney, *Rev. Sci. Instrum.* **2005**, *76*, 023103.
[46] A. G. Marshall, T. C. L. Wang, T. L. Ricca, *J. Am. Chem. Soc.* **1985**, *107*, 7893.
[47] Gaussian 03, (Revision C.02), M. J. Frisch, G. W. Trucks, H. B. Schlegel, G. E. Scuseria, M. A. Robb, J. R. Cheeseman, J. A. Montgomery, Jr., T. Vreven, K. N. Kudin, J. C. Burant, J. M. Millam, S. S. Iyengar, J. Tomasi, V. Barone, B. Mennucci, M. Cossi, G. Scalmani, N. Rega, G. A. Petersson, H. Nakatsuji, M. Hada, M. Ehara, K. Toyota, R. Fukuda, J. Hasegawa, M. Ishida, T. Nakajima, Y. Honda, O. Kitao, H. Nakai, M. Klene, X. Li, J. E. Knox, H. P. Hratchian, J. B. Cross, C. Adamo, J. Jaramillo, R. Gomperts, R. E. Stratmann, O. Yazyev, A. J. Austin, R. Cammi, C. Pomelli, J. W. Ochterski, P. Y. Ayala, K. Morokuma, G. A. Voth, P. Salvador, J. J. Dannenberg, V. G. Zakrzewski, S. Dapprich, A. D. Daniels, M. C. Strain, O. Farkas, D. K. Malick, A. D. Rabuck, K. Raghavachari, J. B. Foresman, J. V. Ortiz, Q. Cui, A. G. Baboul, S. Clifford, J. Cioslowski, B. B. Stefanov, G. Liu, A. Liashenko, P. Piskorz, I. Komaromi, R. L. Martin, D. J. Fox, T. Keith, M. A. Al-Laham, C. Y. Peng, A. Nanayakkara, M. Challacombe, P. M. W. Gill, B. Johnson, W. Chen, M. W. Wong, C. Gonzalez, J. A. Pople, Gaussian, Inc., Wallingford, CT, **2004**.
[48] A. D. Becke, *J. Chem. Phys.* **1993**, *98*, 5648.
[49] A. D. Becke, *J. Chem. Phys.* **1996**, *104*, 1040.
[50] C. T. Lee, W. T. Yang, R. G. Parr, *Phys. Rev. B* **1988**, *37*, 785.
[51] M. P. Andersson, P. Uvdal, *J. Phys. Chem. A* **2005**, *109*, 2937.

Received: February 18, 2011
Published online on May 25, 2011

